CD28 and CD3 have complementary roles in T-cell traction forces

Keenan T. Bashour[a], Alexander Gondarenko[b], Haoqian Chen[a], Keyue Shen[a], Xin Liu[c], Morgan Huse[c], James C. Hone[b], and Lance C. Kam[a,1]

Departments of [a]Biomedical Engineering and [b]Mechanical Engineering, Columbia University, New York, NY 10027; and [c]Immunology Program, Memorial Sloan–Kettering Cancer Center, New York, NY 10065

Edited by Ellis L. Reinherz, Dana–Farber Cancer Institute, Boston, MA, and accepted by the Editorial Board January 4, 2014 (received for review August 16, 2013)

Mechanical forces have key roles in regulating activation of T cells and coordination of the adaptive immune response. A recent example is the ability of T cells to sense the rigidity of an underlying substrate through the T-cell receptor (TCR) coreceptor CD3 and CD28, a costimulation signal essential for cell activation. In this report, we show that these two receptor systems provide complementary functions in regulating the cellular forces needed to test the mechanical properties of the extracellular environment. Traction force microscopy was carried out on primary human cells interacting with micrometer-scale elastomer pillar arrays presenting activation antibodies to CD3 and/or CD28. T cells generated traction forces of 100 pN on arrays with both antibodies. By providing one antibody or the other in solution instead of on the pillars, we show that force generation is associated with CD3 and the TCR complex. Engagement of CD28 increases traction forces associated with CD3 through the signaling pathway involving PI3K, rather than providing additional coupling between the cell and surface. Force generation is concentrated to the cell periphery and associated with molecular complexes containing phosphorylated Pyk2, suggesting that T cells use processes that share features with integrin signaling in force generation. Finally, the ability of T cells to apply forces through the TCR itself, rather than the CD3 coreceptor, was tested. Mouse cells expressing the 5C.C7 TCR exerted traction forces on pillars presenting peptide-loaded MHCs that were similar to those with α-CD3, suggesting that forces are applied to antigen-presenting cells during activation.

T-cell activation is a key regulatory point of the adaptive immune response. It is initiated by recognition of peptide-loaded MHCs (pMHCs) on antigen-presenting cells (APCs) by T-cell receptors (TCRs). Engagement of additional receptors on the T-cell surface leads to formation of a specialized interface termed the immune synapse (IS), which focuses communication between these cells. The IS has emerged as a compelling model of juxtacrine signaling, providing key insights into how the dynamics of such interfaces influence cell–cell communication. Mechanical forces originating from a range of sources, including cytoskeletal dynamics, also play important roles in T-cell activation. The initial spreading of T cells following contact with an activating surface is dependent on a burst of actin polymerization (1, 2). Subsequent retrograde flow of actin and contraction of actomyosin structures drive microscale reorganization of signaling complexes within this interface, resulting in formation of concentric central, peripheral, and distal supramolecular activation cluster (cSMAC, pSMAC, and dSMAC) structures that comprise the archetypal IS (3–8). The TCR complex itself may be triggered by external forces (9, 10), whereas TCR ligation may induce actin polymerization and generation of protrusive forces (11).

More recently, mechanosensing by T cells was demonstrated in the context of CD28 costimulation (12, 13). Activating antibodies to CD3 (epsilon chain) and CD28, which provide antigen-independent signaling of the TCR complex and costimulation, respectively (14–16), were attached to polymer and hydrogel supports and presented to primary T cells. Multiple cellular functions, including Interleukin-2 (IL-2) secretion and proliferation, responded to the rigidity of the substrate, echoing the phenomenon of mechanosensing observed in other types of cells interacting with ECM. Notably, CD3 and CD28 share little in common with integrins, and understanding how CD3 and CD28 facilitate rigidity sensing, particularly with regard to generation of cellular forces needed to test the extracellular environment, would shed new light on mechanobiology. In this direction, this report seeks to understand the mechanical state of T-cell interfaces formed in response to CD3 and CD28 engagement and to identify the roles each signaling system has in this interaction. Primary human $CD4^+$ T cells will be the main focus of this study, given their utility in cellular immunotherapy and their demonstrated ability to respond to substrate rigidity (13).

Results

Human Primary T Cells Generate Traction Forces on Surfaces Engaging CD3 and CD28. T-cell traction forces were measured using elastomer pillar arrays as the cell culture surface (Fig. 1*A*). In this approach, the deflection of each pillar tip is followed by live-cell microscopy and used to provide a spatially resolved map of forces (17, 18). A standard geometry of 1-μm diameter, 6-μm tall pillars arranged 2 μm center to center in hexagonal arrays was used unless otherwise stated. The arrays were composed of Sylgard 184 polydimethylsiloxane (PDMS), resulting in a spring constant (17) of 1.4 nN/μm, allowing sufficient deflection to estimate forces while avoiding interpillar collisions. Arrays were coated with the antibodies OKT3 and CD28.6, which activate

Significance

Cells have the remarkable ability to sense the mechanical properties of the extracellular environment. This has been developed primarily in the context of cell interaction with extracellular matrix through integrins, but recent studies showed that T cells exhibit mechanosensing through CD3 and CD28, nonintegrin receptors that provide activation and costimulatory signals. This report demonstrates that T cells generate significant forces through the T-cell receptor (TCR) and CD28, and delineates the contributions of each in force generation. Moreover, the distribution of force generation and local assembly of active signaling intermediates suggest similarities between TCR- and integrin-based connections between the cell and substrate.

Author contributions: K.T.B., H.C., K.S., M.H., J.C.H., and L.C.K. designed research; K.T.B., A.G., H.C., K.S., and X.L. performed research; A.G., X.L., M.H., and J.C.H. contributed new reagents/analytic tools; K.T.B., A.G., H.C., K.S., X.L., and L.C.K. analyzed data; and K.T.B. and L.C.K. wrote the paper.

The authors declare no conflict of interest.

This article is a PNAS Direct Submission. E.L.R. is a guest editor invited by the Editorial Board.

[1]To whom correspondence should be addressed. E-mail: lk2141@columbia.edu.

This article contains supporting information online at www.pnas.org/lookup/suppl/doi:10.1073/pnas.1315606111/-/DCSupplemental.

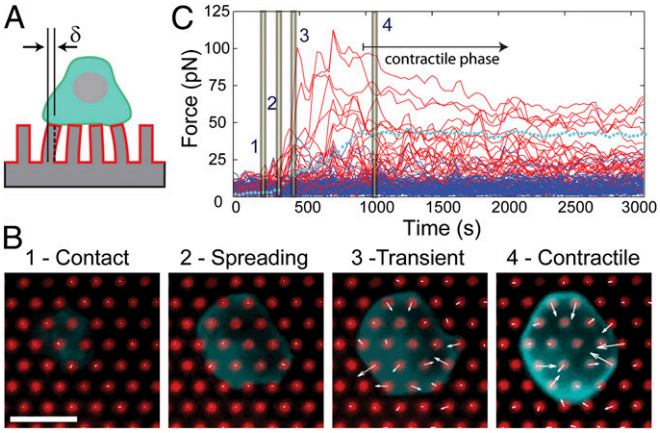

Fig. 1. Contractile forces on pillar arrays. (*A*) T-cell traction forces were measured using elastomer pillar arrays. (*B*) T cells (cyan) interacting with pillar arrays coated with OKT3 + CD28.6 (red) show four distinct phases: *1*) initial contact; *2*) rapid spreading; *3*) transient, uncoordinated force generation; and *4*) stable contraction. The contractile phase typically begins within 20 min of seeding and lasts the duration of imaging, 1 h. Scale bar: 5 μm and 250 pN (forces are indicated as arrows). This scaling between distance and force is for presentation only and does not indicate the actual pillar displacement. Additional cells are included in Movies S1–S3. (*C*) Representative plot of the magnitude of force applied to individual pillars as a function of time. Red traces indicate forces on individual pillars under the cell, whereas the blue traces represent pillars away from the interface. The dotted cyan line indicates the average pillar force within the cell–array interface. Time points corresponding to the images in *B* are indicated by numbers 1–4.

CD3 and CD28, respectively. A fraction of these antibodies was labeled to allow pillar tracking by fluorescence, avoiding distortions from cells that may occur with transmitted light (details and characterization are included in *Materials and Methods*).

Primary human $CD4^+$ T cells undergo a dynamic, multiphase interaction with these arrays that resembles that seen on other substrates (4, 8, 15). The progression of a representative cell through these phases is shown in Fig. 1 *B* and *C*, and additional examples are included as *Supporting Information* (Movies S1–S3). Upon contacting the arrays, cells rapidly spread across multiple pillars (Fig. 1*B*, Movie S1). This phase results from engagement of the TCR complex, as spreading was observed on pillars coated with OKT3 alone (Movie S2); conversely, few cells attached to arrays coated with only CD28.6. During this rapid spreading phase, cells generated only minor forces, which were similar to the fluctuations observed for pillars outside this interface (Fig. 1 *B* and *C*, Movie S3). The area of this interface stabilizes over the next minutes (Fig. 1 *B* and *C*), similar to the cessation of spreading observed on lipid bilayers and solid supports, which is followed by centripetal transport of microclusters across the IS. On the pillar arrays, significant traction forces begin to be generated as the cell interface stabilizes, passing through a short transient phase during which forces are uncoordinated (Fig. 1 *B* and *C*, Movie S3) and entering a sustained, contractile phase in which forces are predominantly centripetal in direction and strongest along the cell periphery (Fig. 1 *B* and *C*, Movie S3). Cells entered this contractile phase within 20 min of contact with the pillar arrays. Given the importance of sustained synapse function in T-cell activation (19, 20), comparisons later in this report focus on this contractile phase. However, we first verified activation of T cells on micropillar arrays, using IL-2 as a functional marker. Secretion of this cytokine was measured using a surface-capture technique (21) that provides a relative comparison between conditions. IL-2 secretion on arrays coated with OKT3 + CD28.6 (CoStim; Fig. 2*A*) was almost two orders of magnitude greater than that on arrays with OKT3 alone (Fig. 2*A*). Furthermore, IL-2 secretion on pillars coated with OKT3 + CD28.6 was similar to that on flat PDMS, indicating that these arrays provide functional, CD28-dependent activation of T cells.

Focusing next on the contractile phase, $CD4^+$ T cells on surfaces coated with OKT + CD28.6 developed traction forces that peaked in the range of 100 pN (Fig. 1*B*), small compared with the nano-Newton forces associated with integrin–ECM interactions (17). However, traction forces may respond to the stiffness of the underlying substrate; Saez et al. (22) showed that epithelial cells induce a specific deflection of fibronectin-coated pillars independent of spring constant, applying larger forces to pillars as stiffness increases. To determine whether a similar phenomenon explains the small forces observed here, pillar height was varied while keeping other dimensions constant. The magnitude of force applied to all pillars underlying the cell was averaged over 20 min of the contractile phase, providing a single measure of traction force generation. On pillars of 6 μm height, cells exerted an average, per pillar force of 73.8 ± 29.1 pN (mean ± SD, $n > 30$ cells). Changing pillar height from 5 to 8 μm altered neither the average force nor the number of pillars in contact with each T cell (Fig. 2*B*), indicating that T-cell traction forces are not sensitive to pillar stiffness.

CD28 Costimulation Augments Traction Forces Generated Through CD3. CD28 and TCR signaling converge through a complex network of phosphorylation cascades and other intermediate biomolecules. To understand the role of each receptor in force generation, we first examined cells on arrays coated with OKT3 alone. T cells generated per pillar forces of 41.4 ± 18.1 pN (mean ± SD, $n = 22$ cells), about half that on OKT3 + CD28.6, whereas the number of pillars in contact with each cell was not affected (Fig. 2*C*). As shown in Fig. 2*D*, this lower average force was associated with a decrease in force applied to each pillar rather than a loss in the number of pillars experiencing strong forces. Cells were seeded onto pillars coated with CD28.6 alone, but as noted earlier, these surfaces did not support significant cell adhesion; it was not possible to obtain representative force measurements without concurrent CD3 engagement. Instead, cells were seeded onto pillars coated with only OKT3 whereas CD28.6 was included in the cell culture media. Traction forces in this configuration were not significantly different from substrates coated with OKT3 + CD28.6 (Fig. 2*C*), indicating that force generation occurs through the TCR complex. CD28 increases traction forces through intracellular signaling as opposed to providing additional traction through this costimulatory receptor. To delineate these signaling pathways, we examined phosphoinositide 3-kinase (PI3K), which binds to the cytosolic domain of CD28, leading to conversion of PIP_2 to PIP_3, activation of PKB (Akt) and phosphoinositide-dependent kinase 1 (PDK1), and subsequent signaling (16, 23, 24) (Fig. 2 *C* and *E*). Cells were seeded on pillars coated with OKT3 + CD28.6, followed 15 min later by wash-in of select pharmacological inhibitors. The PI3K inhibitor 17β-hydroxy wortmannin (HWT) reduced T-cell traction forces on arrays coated with OKT3 + CD28.6 to levels comparable with that on OKT3 alone (Fig. 2*C*). Similar to that observed on the OKT3 surface, HWT reduced the magnitude of forces applied to each pillar (Fig. 2*D*). Traction forces on arrays coated with only OKT3 were not affected by HWT wash-in (Fig. 2*C*), indicating that although PI3K also is downstream of TCR, it is not involved in signaling related to traction forces generated through this membrane protein. Downstream of PI3K, inhibition of Akt with triciribine (Tric) did not affect traction forces on arrays coated with OKT3 + CD28.6 (Fig. 2*C*). Application of the PDK1 inhibitor GSK2334470 (GSK) (25, 26) completely abrogated force generation in T cells (Fig. 2*C*), suggesting that PDK1 modulates force generation downstream from CD28. However, PDK1 integrates CD28 and CD3 signaling (27), and the reduction of forces by GSK2334470 likely reflects inhibition of both pathways.

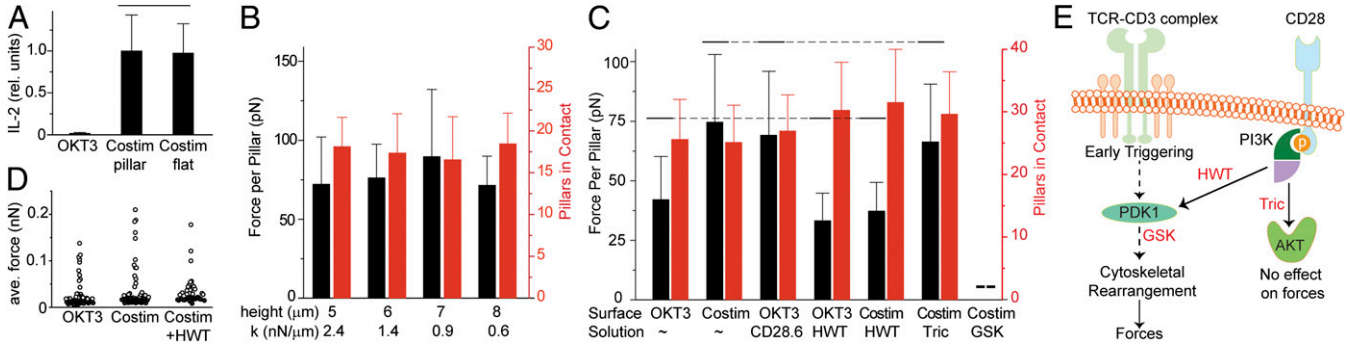

Fig. 2. Traction forces are insensitive to pillar height but respond to CD28 costimulation. (*A*) Engagement of CD28 augments CD3 signaling, providing functional activation of T cells as measured by 6-h secretion of IL-2. Costim: OKT3 + CD28.6. Data are mean ± SD from three independent experiments; each experiment is represented by the average staining for IL-2 collected over more than 300 cells per condition. Overbars group conditions that were not significantly different, as analyzed using ANOVA and Tukey multiple comparison methods, $\alpha = 0.05$. (*B*) The average force and number of pillars contacting a cell on arrays coated with OKT3 + CD28.6 was independent of spring constant. Data are mean ± SD, representing 7–13 cells for each height from three independent experiments, and were analyzed by ANOVA, $\alpha = 0.05$; overbars are omitted, as no difference was observed. (*C*) Delineation of pathways through which CD28 augments cellular forces. Data are mean ± SD, from 18–43 cells for each condition over three independent experiments. Solid overbars connected by dotted lines group conditions that were not statistically different, $\alpha = 0.05$. Overbars are omitted for data of pillars engaged by cells, as no difference was observed between conditions. (*D*) Average traction force per pillar during the contractile phase from a representative cell for each condition. ●, Pillars away from the cell; ○, pillars underlying the cell. (*E*) Schematic of force augmentation by CD28 signaling. Inhibitors are indicated in red.

Sustained Src Family Kinase Signaling Is Required for CD3-Based Traction Forces. Having identified TCR/CD3 as the source of traction forces, this section focuses on identifying molecular complexes that locally regulate force generation through the TCR complex. T cells were seeded on arrays coated with OKT3 + CD28.6, then fixed during the contractile stage. A pillar height of 8 μm was used in these experiments to allow clearer measurement of tip deflection. Phalloidin staining revealed an F-actin network that spanned the cell interface but was concentrated at the cell periphery (Fig. 3*A*). Myosin IIA also was distributed across the interface, with a higher concentration in the cell periphery (Fig. 3*A*); the basic machinery for contractile force generation is found throughout the interface. The pillars also altered the local distributions of both proteins, producing rings of actin around individual pillars and a depletion of myosin IIA on top of each structure (Fig. 3*A*). Similar perturbations have been observed in fibroblasts interacting with ECM-coated pillars (28), but the implications of these local changes remain unclear. As a mechanism for regulating contractility, we focused on proline-rich tyrosine kinase 2 (Pyk2), which is related to focal adhesion kinase (FAK) but restricted to neuronal, epithelial, and hematopoietic cells. TCR stimulation leads to Pyk2 phosphorylation, recruitment, and activation of cytoskeletal reorganization (29–32). In particular, Pyk2 phosphorylation on Tyr-402 is required for full activation (30). Phosphospecific staining for this active form (pPyk2) was localized to the pillar tops, preferentially those at the periphery of the cell, where the largest forces also are found (Fig. 3*B*). The distribution of pPyk2 around each pillar largely was asymmetric, with accumulation around the edge away from the cell center, although pillars completely encircled by pPyk2 also were observed (Fig. 3*B*). Quantitatively, a moderate level of correlation was found between pPyk2 staining (measured and compared as described in *Materials and Methods*) and applied force (Spearman's rank correlation coefficient, $R_S = 0.49$;

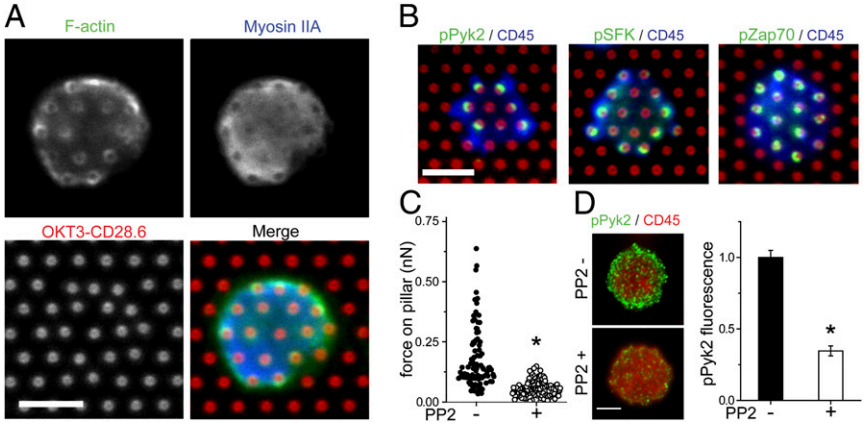

Fig. 3. Local assembly of proteins regulates traction forces. (*A*) F-actin (green in merged image) and myosin IIA (blue) are present throughout the T-cell–array interface but concentrated in the cell periphery. Pillars were coated with OKT3 + CD28.6 (red). Cells were fixed 30 min after seeding. Scale bar: 5 μm. (*B*) Phosphospecific staining showed localization of pPyk2 (green, *Left*) and pSFK (green, *Center*) to the periphery of the cell–array interface. Phospho-Zap70 (green, *Right*) did not show this preferential localization. Cell morphology was visualized using anti-CD45 Fab fragments (blue). Scale bar: 5 μm. (*C*) Wash-in of the SFK inhibitor PP2 reduces traction forces. Data represent at least 90 pillars from eight cells over two independent experiments for each condition. $^*P <$ 0.05 compared with no PP2, dual-tailed *t* test. (*D*) PP2 treatment reduced overall intensity of pPyk2 staining on planar PDMS coated with OKT3 + CD28.6. Control and inhibited samples were imaged in parallel for each experiment, and normalized to the noninhibited condition. Data are mean ± SD from >200 cells per surface, from more than three independent experiments. $^*P < 0.05$ compared with no PP2.

Fig. S1*A*), suggesting a role of Pyk2 in modulating cellular forces. We next focused on the Src family kinases (SFKs) lymphocyte-specific kinase (Lck) and Fyn, which are the main members expressed in T cells, act as downstream effectors of TCR signaling, and modulate Pyk2 function. For example, Lck/Fyn activity mediates translocation of Pyk2 to the IS in response to TCR stimulation (31, 33). Binding of Tyr-402–phosphorylated Pyk2 by Lck and/or Fyn also leads to phosphorylation of additional sites on this protein, further enhancing kinase function (29, 30). Staining with a phosphospecific antibody (pSFK) that recognizes the homologous activation sites of both Lck (Tyr-393) and Fyn (Tyr-416) was preferentially localized to pillars at the periphery of the T-cell–array interface, similar to pPyk2 (Fig. 3*B*). Also, like pPyk2, pSFK staining showed a moderate correlation with pillar deflection (R_S = 0.50; Fig. S1*B*), suggesting a link between these proteins and force generation. In contrast to pSFK and pPyk2, staining for Tyr-319–phosphorylated zeta-chain–associated protein kinase 70 (Zap70) was distributed widely across pillars, including those underlying the center of the cell, and exhibited no correlation with pillar deflection (Fig. 3*B* and Fig. S1*A*; R_S = −0.165). The contrasting distributions of pZap70 and pPyk2 reinforce the concept that different products of SFK signaling have varying roles in T-cell function, not all of which are associated with force generation. To further assess the roles of SFK in force generation, the kinase inhibitor PP2 (34) was washed in 10 min after cell seeding, which allowed time for cells to adhere and begin exerting contractile forces. Over the subsequent 15–20 min of PP2 exposure, pillar displacements decreased by 70% (Fig. 3*C*), indicating that SFK signaling is needed for sustained force generation. PP2 treatment also decreased pPyk2 staining on the pillar arrays, to an extent to which measuring normalized fluorescence intensity on individual pillars was hindered by the low signals involved. We instead treated cells on flat areas of PDMS, coated with OKT3 + CD28.6, with PP2. PP2 significantly decreased the presence of pPyk2 along the cell periphery and the overall signal across the interface (Fig. 3*D*). Together with the observed correlation between force generation and pPyk2 staining (Fig. S1*A*), this result suggests that Pyk2 is associated with signaling that leads to local force generation, downstream of Lck/Fyn.

Cells Apply Force Through the TCR. Initiation of TCR through an α-CD3 antibody bypasses antigen recognition, allowing studies of primary human T cells displaying their normal repertoire of TCRs, but does not capture the physiological TCR–pMHC interaction. Given the comparatively low affinity of TCR–pMHC compared with CD3 antibody, it is reasonable to expect that T cells would not exert significant forces on pMHCs. To test this possibility, the pillar array system was modified to present an I-Ek MHC loaded with moth cytochrome C (MCC) peptide, which is recognized by mouse T cells expressing the 5C.C7 transgenic TCR. Specifically, arrays were coated with streptavidin, which then was used to capture biotinylated pMHC. Activating antibodies to CD28 were included in solution to isolate forces associated with the TCR–pMHC interaction. In comparison with primary human cells, interfaces formed by mouse cells on pillar arrays coated with α-CD3 are smaller, encompassing fewer pillars (Fig. 4 *A* and *B*). The forces produced by mouse cells on α-CD3–coated pillars are on the order of 200 pN (Fig. 4*B*), larger than that associated with human cells (Fig. 2*C*), potentially reflecting differences in affinity between the species-specific α-CD3 antibodies. Replacing α-CD3 with pMHC did not change the per pillar force or number of pillars engaged by the cell (Fig. 4*B*), suggesting that these cells can generate significant forces through the TCR. Cells exhibited minimal adhesion to arrays presenting only pMHC (in the absence of α-CD28), and for the few that did attach, the deflections of pillars underlying the cells were indistinguishable from background pillars. Lastly, forces generated by cells interacting with

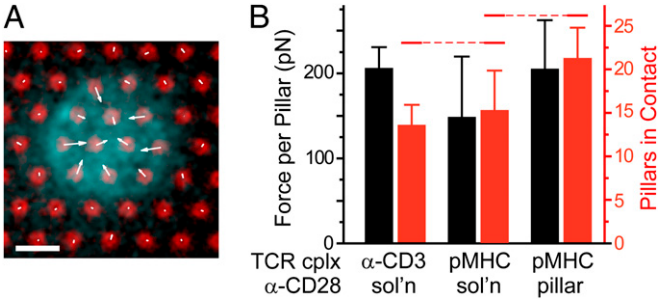

Fig. 4. T cells generate traction forces through TCR–pMHC. (*A*) Primary $CD4^+$ T cell from mouse expressing the 5C.C7 transgenic TCR (cyan, visualized using α-CD45 Fabs) on a pillar array coated with species-appropriate α-CD3 antibody (red); α-CD28 is included in the cell culture media. Scale bar: 2 μm and 500 pN (for forces indicated as arrows). (*B*) Average traction force and number of underlying pillars for cells on surfaces presenting α-CD3 antibody or MCC-loaded I-Ek MHC to target the TCR complex (TCR cplx). CD28 was applied either in solution (sol'n) or coadsorbed onto the pillar. Data are mean ± SD, representing 10–15 cells per condition, and were analyzed using ANOVA and Tukey methods, α = 0.05. Data of force per pillar were not statistically different by ANOVA; grouping overbars are omitted. For data of pillar number, the red overbars group conditions that were not significantly different.

arrays coated with both pMHC and α-CD28 were similar to those for which the costimulatory ligand was presented in solution. Similar to the human cell system, this suggests that CD28 signaling augments forces generated through the TCR complex.

Discussion

A specific function of mechanical forces in T-cell physiology was suggested in early studies of the immune synapse (4). TCR-containing microclusters are transported from the cell periphery, where they form, and toward the central, cSMAC structure (5–8) under the influence of actin polymerization and contraction. Transport of microclusters across the pSMAC has been of particular interest, as limiting this mobility enhances T-cell activation (35, 36). The results reported here suggest that the periphery of the cell–substrate interface, corresponding to the dSMAC described in the other systems, also serves as a platform for mechanical activity, but with functions different from those of the pSMAC, because forces are stronger in this region than in the central area of the interface. This agrees with the model that the dSMAC is analogous to cellular lamellipodia, whereas the pSMAC represents lamella (7, 8). However, it is recognized that these designations may not accurately describe the interaction of T cells with pillar arrays coated with α-CD3 and α-CD28; in particular, this system does not include intercellular adhesion molecule 1 (ICAM-1), which serves as a ligand to lymphocyte function-associated antigen 1 (LFA-1) and in part defines the pSMAC. However, the pillar arrays induce functional activation (Fig. 2*A*), suggesting that our model does share features with the archetypal IS. The choice of CD28 rather than ICAM-1 for this study has additional implications. Unlike CD28, LFA-1 is an integrin receptor and may exhibit its own mechanosensing including requirement of anchorage of ligands to a substrate; the ability of α-CD28 antibodies to act in solution suggests that mechanosensing through CD28 itself is minimal. The focus on CD28 thus provides a strategic means for separating the role of the TCR complex in traction force generation.

The concentration of pPyk2 and pSFK in the cell periphery and around pillars undergoing deflection suggests molecular complexes analogous to focal adhesions, with the TCR acting in place of an integrin. Moreover, CasL, a p130Cas family member expressed in T cells, localizes to the dSMAC (37), associates with FAK/Pyk2 (38), and has been implicated in T-cell mechanics

(37), further supporting the focal adhesion analogy. There are key differences between these systems, however. First, TCR/CD3-based traction forces are lower than those typically associated with integrin–ECM interactions (Figs. 1, 2, and 4), suggesting weaker interactions between these assemblies and the cell cytoskeleton. Studies following retrograde flow in the IS support this scenario, as the speed of TCR microcluster transport on supported lipid bilayers is about half the actin flow speed, and restriction of microcluster transport slows but does not stop actin retrograde flow (39–41). Moreover, immobilization of integrin receptors within the IS slows actin transport to a larger degree than TCR microclusters (39). The second difference is that TCR-associated traction forces are constant over a range of pillar spring constants, unlike that associated with integrin receptors (22, 42). A looser connection between the TCR complex and the cell cytoskeleton, resembling slippage, also might explain this lack of force modulation, reconciling the machinery involved in both systems.

Finally, recent studies identified roles of forces in B-cell activation (43, 44), demonstrating wider application of mechanics in immune cell function. By providing a strategic, comparative system complementary to that developed in the context of integrins or cadherins (45), better understanding of forces in immune cell function promises to significantly advance the field of mechanobiology.

Materials and Methods

Proteins. Studies with human cells used the antibodies OKT3 (317315; BioLegend) and CD28.6 (16–0288; eBioscience). For mouse T cells, antibody clones 145–2C11 and 37.51 (both from eBioscience) were used to activate CD3 and CD28, respectively. Biotinylated I-Ek MHCs, loaded with MCC peptide, were produced in house using established techniques (46) and attached to pillar arrays as described below.

Substrate Fabrication. Arrays of PDMS (Sylgard 184; Dow Corning) pillars and trenches were created following established microfabrication techniques (17), and were cast on thickness #0 glass coverslips (Fisher Scientific) to facilitate imaging. The topology and dimensions of pillar arrays were verified by SEM. Unless otherwise noted, these surfaces consisted of pillars measuring 1 μm in diameter and 5–9 μm in height and spaced in hexagonal arrays at a 2-μm center-to-center distance. Costimulatory pillar arrays for use with human cells were coated for 2 h at 37 °C with OKT3 and CD28.6 at a concentration of 5 μg/mL each. For surfaces coated with OKT3 alone, the concentration of this antibody was doubled to 10 μg/mL. Arrays then were blocked with 4% (wt/vol) BSA for 2 h before use in cell experiments. Arrays to be used with mouse cells were coated with 20 μg/mL of either α-CD3 or streptavidin. For presentation of both TCR and CD28 ligands on the pillars, these arrays were coated with 10 μm/mL each of streptavidin and α-CD28, followed by capture of biotinylated I-Ek. pMHCs were captured onto streptavidin-coated pillars by incubating the substrate with 100 μg/mL of MCC-loaded I-Ek. When presented in solution, α-CD28 antibodies were at a concentration of 10 μg/mL.

T-Cell Isolation and Culture. Human resting primary T cells were prepared following protocols approved by the Columbia Institutional Review Board; $CD4^+$ T cells were enriched from peripheral blood mononuclear cell preparations by negative isolation (Dynabeads Untouched $CD4^+$ T cells; Invitrogen). Cell culture media consisted of RPMI-1640 media supplemented with 10% (vol/vol) FBS, 2 mM L-glutamine, 10 mM Hepes, 50 μM β-mercaptoethanol, 50 U/mL penicillin, and 50 μg/mL streptomycin. Cells were seeded at 5,000 cells/mm^2 and maintained at 37 °C, 5% (vol/vol) CO_2 for the specified times. For inhibition studies, reagents were washed in 15 min after cell–substrate contact. Inhibitors were applied at the following concentrations: HWT = 50 nM, Tric = 10 μM, GSK = 10 nM. For wash-in of SFK inhibitors, PP2 was applied at 20 μM. Naïve $CD4^+$ T cells were isolated from lymph nodes of Rag2 knockout Cyt5C.C7 mice by negative selection (Dynal CD4 Negative Isolation Kit; Invitrogen). These cells were cultured in RPMI-1640 supplemented with 5% (vol/vol) mouse serum and used at a density of 2×10^4 cells/mm^2 immediately after isolation.

Quantification of Cellular Forces. Cell traction forces were calculated from the deflection of individual pillar tips (17, 18). To facilitate fluorescence-based imaging of the pillars, a small fraction (1:5) of the OKT3 antibody was labeled with amine-reactive Alexa 647 (Invitrogen). Images for measurement of forces during sustained contraction were collected for 20 min, starting 20 min after seeding. Pillars outside the cell–array contact area were used to correct for drift and stage movement. The ImageJ software package then was used to track pillar deflections, which then were converted to net forces as described by Schoen et al. (18). The pillars exhibited limited movement in the cell culture environment, even in the absence of adherent cells. For the standard pillars of 6 μm height and 1 μm diameter, the time-averaged force corresponding to these background pillars was 5 pN, which we adopt as the accuracy of time-averaged measurements and the minimum force detectable in this study.

Immunostaining. For studies of protein localization, cells were fixed 30 min after seeding with 4% (wt/vol) paraformaldehyde, permeabilized with 0.1% Triton X-100 in PBS, and stained using standard techniques. Staining was carried out using primary antibodies against CD45 (304019; BioLegend), Pyk2 (Poly6053; BioLegend), phosphorylated Zap70 Tyr-319 (2701S; Cell Signaling), phosphorylated Lck Tyr-394 (NBP1-60894; Novus Biologics), phosphorylated Pyk2 Tyr-402 (44–618G; Invitrogen), or nonmuscle myosin IIA (ab24762; Abcam), followed by appropriate secondary antibodies conjugated with Alexa fluorophores (Invitrogen). Cells also were stained for actin cytoskeleton using phalloidin (A12379; Invitrogen). For live-cell imaging of cell morphology, F_{AB} fragments of anti-CD45 were used to track the cell membrane. Protein localization vs. applied force was compared quantitatively by measuring the average fluorescence intensity inside a 1.1-μm diameter circle centered on each pillar tip. This was normalized to the average staining measured across the entire cell interface, which included all other pillars underlying the cell. A value of 0 for this normalized fluorescence indicates no staining on the pillar top. Larger values represent stronger staining.

Cytokine Secretion. Assays of IL-2 secretion were carried out using an established surface-capture method (12, 21, 47). Briefly, cells were incubated with an IL-2 capture reagent from a secretion assay kit (Miltenyi Biotec) before seeding. One hour after seeding, samples were rinsed with warm (37° C) RPMI-1640 medium. After an additional 5 h of incubation, cells were rinsed and incubated with a fluorescently labeled antibody to IL-2. The per cell fluorescence intensity associated with APC-labeled IL-2 (presented in arbitrary units) was measured by fluorescence microscopy. All samples to be compared were included in each experiment, and all were stained, imaged, and processed in the same session to allow comparison among samples.

Statistics Analysis. Multiple conditions were compared first by ANOVA then, when statistical significance was indicated, using Tukey's honest significant difference (HSD) criteria. Data of pillar displacement vs. staining enrichment were carried out using the nonparametric Spearman rank correlation coefficient, R_s. Like the parametric Pearson correlation coefficient, R_s may range from −1 to 1, representing complete negative and positive correlation. A value of 0 indicates no correlation. Unless otherwise noted, statistical tests were carried out using a significance level $\alpha = 0.05$.

ACKNOWLEDGMENTS. This work is supported by the National Institutes of Health (PN2EY016586, R01AI088377, R01AI087644, and R21EB008199) and the National Science Foundation (Integrative Graduate Education and Research Traineeship award 0801530).

1. Barda-Saad M, et al. (2005) Dynamic molecular interactions linking the T cell antigen receptor to the actin cytoskeleton. *Nat Immunol* 6(1):80–89.
2. Gomez TS, et al. (2007) Formins regulate the actin-related protein 2/3 complex-independent polarization of the centrosome to the immunological synapse. *Immunity* 26(2):177–190.
3. DeMond AL, Mossman KD, Starr T, Dustin ML, Groves JT (2008) T cell receptor microcluster transport through molecular mazes reveals mechanism of translocation. *Biophys J* 94(8):3286–3292.
4. Grakoui A, et al. (1999) The immunological synapse: A molecular machine controlling T cell activation. *Science* 285(5425):221–227.
5. Ilani T, Vasiliver-Shamis G, Vardhana S, Bretscher A, Dustin ML (2009) T cell antigen receptor signaling and immunological synapse stability require myosin IIA. *Nat Immunol* 10(5):531–539.
6. Kaizuka Y, Douglass AD, Varma R, Dustin ML, Vale RD (2007) Mechanisms for segregating T cell receptor and adhesion molecules during immunological synapse formation in Jurkat T cells. *Proc Natl Acad Sci USA* 104(51):20296–20301.

7. Kumari S, et al. (2012) T lymphocyte myosin IIA is required for maturation of the immunological synapse. *Front Immunol* 3:230.
8. Babich A, et al. (2012) F-actin polymerization and retrograde flow drive sustained PLCγ1 signaling during T cell activation. *J Cell Biol* 197(6):775–787.
9. Li YC, et al. (2010) Cutting edge: Mechanical forces acting on T cells immobilized via the TCR complex can trigger TCR signaling. *J Immunol* 184(11):5959–5963.
10. Kim ST, et al. (2009) The alphabeta T cell receptor is an anisotropic mechanosensor. *J Biol Chem* 284(45):31028–31037.
11. Husson J, Chemin K, Bohineust A, Hivroz C, Henry N (2011) Force generation upon T cell receptor engagement. *PLoS One* 6(5):e19680.
12. Judokusumo E, Tabdanov E, Kumari S, Dustin ML, Kam LC (2012) Mechanosensing in T lymphocyte activation. *Biophys J* 102(2):L5–L7.
13. O'Connor RS, et al. (2012) Substrate rigidity regulates human T cell activation and proliferation. *J Immunol* 189(3):1330–1339.
14. Sedwick CE, et al. (1999) TCR, LFA-1, and CD28 play unique and complementary roles in signaling T cell cytoskeletal reorganization. *J Immunol* 162(3):1367–1375.
15. Bromley SK, et al. (2001) The immunological synapse and CD28-CD80 interactions. *Nat Immunol* 2(12):1159–1166.
16. Riha P, Rudd CE (2010) CD28 co-signaling in the adaptive immune response. *Self Nonself* 1(3):231–240.
17. Tan JL, et al. (2003) Cells lying on a bed of microneedles: an approach to isolate mechanical force. *Proc Natl Acad Sci USA* 100(4):1484–1489.
18. Schoen I, Hu W, Klotzsch E, Vogel V (2010) Probing cellular traction forces by micropillar arrays: Contribution of substrate warping to pillar deflection. *Nano Lett* 10(5):1823–1830.
19. Huppa JB, Gleimer M, Sumen C, Davis MM (2003) Continuous T cell receptor signaling required for synapse maintenance and full effector potential. *Nat Immunol* 4(8): 749–755.
20. Iezzi G, Karjalainen K, Lanzavecchia A (1998) The duration of antigenic stimulation determines the fate of naive and effector T cells. *Immunity* 8(1):89–95.
21. Shen K, Thomas VK, Dustin ML, Kam LC (2008) Micropatterning of costimulatory ligands enhances CD4+ T cell function. *Proc Natl Acad Sci USA* 105(22):7791–7796.
22. Saez A, Buguin A, Silberzan P, Ladoux B (2005) Is the mechanical activity of epithelial cells controlled by deformations or forces? *Biophys J* 89(6):L52–L54.
23. Boomer JS, Green JM (2010) An enigmatic tail of CD28 signaling. *Cold Spring Harb Perspect Biol* 2(8):a002436.
24. Sanchez-Lockhart M, et al. (2004) Cutting edge: CD28-mediated transcriptional and posttranscriptional regulation of IL-2 expression are controlled through different signaling pathways. *J Immunol* 173(12):7120–7124.
25. Najafov A, Shpiro N, Alessi DR (2012) Akt is efficiently activated by PIF-pocket- and PtdIns(3,4,5)P3-dependent mechanisms leading to resistance to PDK1 inhibitors. *Biochem J* 448(2):285–295.
26. Najafov A, Sommer EM, Axten JM, Deyoung MP, Alessi DR (2011) Characterization of GSK2334470, a novel and highly specific inhibitor of PDK1. *Biochem J* 433(2):357–369.
27. Park S-G, et al. (2009) The kinase PDK1 integrates T cell antigen receptor and CD28 coreceptor signaling to induce NF-kappaB and activate T cells. *Nat Immunol* 10(2): 158–166.
28. Ghassemi S, et al. (2012) Cells test substrate rigidity by local contractions on submicrometer pillars. *Proc Natl Acad Sci USA* 109(14):5328–5333.
29. Collins M, Bartelt RR, Houtman JCD (2010) T cell receptor activation leads to two distinct phases of Pyk2 activation and actin cytoskeletal rearrangement in human T cells. *Mol Immunol* 47(9):1665–1674.
30. Ostergaard HL, Lysechko TL (2005) Focal adhesion kinase-related protein tyrosine kinase Pyk2 in T-cell activation and function. *Immunol Res* 31(3):267–282.
31. Sancho D, et al. (2002) TCR engagement induces proline-rich tyrosine kinase-2 (Pyk2) translocation to the T cell-APC interface independently of Pyk2 activity and in an immunoreceptor tyrosine-based activation motif-mediated fashion. *J Immunol* 169(1): 292–300.
32. Beinke S, et al. (2010) Proline-rich tyrosine kinase-2 is critical for CD8 T-cell short-lived effector fate. *Proc Natl Acad Sci USA* 107(37):16234–16239.
33. Collins M, et al. (2010) The T cell receptor-mediated phosphorylation of Pyk2 tyrosines 402 and 580 occurs via a distinct mechanism than other receptor systems. *J Leukoc Biol* 87(4):691–701.
34. Hanke JH, et al. (1996) Discovery of a novel, potent, and Src family-selective tyrosine kinase inhibitor. Study of Lck- and FynT-dependent T cell activation. *J Biol Chem* 271(2):695–701.
35. Maruthamuthu V, Aratyn-Schaus Y, Gardel ML (2010) Conserved F-actin dynamics and force transmission at cell adhesions. *Curr Opin Cell Biol* 22(5):583–588.
36. Mossman KD, Campi G, Groves JT, Dustin ML (2005) Altered TCR signaling from geometrically repatterned immunological synapses. *Science* 310(5751):1191–1193.
37. Hsu CJ, et al. (2012) Ligand mobility modulates immunological synapse formation and T cell activation. *PLoS One* 7(2):e32398.
38. Yu Y, Fay NC, Smoligovets AA, Wu HJ, Groves JT (2012) Myosin IIA modulates T cell receptor transport and CasL phosphorylation during early immunological synapse formation. *PLoS One* 7(2):e30704.
39. Lakkakorpi PT, et al. (1999) Stable association of PYK2 and p130(Cas) in osteoclasts and their co-localization in the sealing zone. *J Biol Chem* 274(8):4900–4907.
40. Nguyen K, Sylvain NR, Bunnell SC (2008) T cell costimulation via the integrin VLA-4 inhibits the actin-dependent centralization of signaling microclusters containing the adaptor SLP-76. *Immunity* 28(6):810–821.
41. Smoligovets AA, Smith AW, Wu HJ, Petit RS, Groves JT (2012) Characterization of dynamic actin associations with T-cell receptor microclusters in primary T cells. *J Cell Sci* 125(Pt 3):735–742.
42. Yu CH, Wu H-J, Kaizuka Y, Vale RD, Groves JT (2010) Altered actin centripetal retrograde flow in physically restricted immunological synapses. *PLoS One* 5(7):e11878.
43. Bangasser BL, Rosenfeld SS, Odde DJ (2013) Determinants of maximal force transmission in a motor-clutch model of cell traction in a compliant microenvironment. *Biophys J* 105(3):581–592.
44. Natkanski E, et al. (2013) B cells use mechanical energy to discriminate antigen affinities. *Science* 340(6140):1587–1590.
45. Wan Z, et al. (2013) B cell activation is regulated by the stiffness properties of the substrate presenting the antigens. *J Immunol* 190(9):4661–4675.
46. Huse M, et al. (2007) Spatial and temporal dynamics of T cell receptor signaling with a photoactivatable agonist. *Immunity* 27(1):76–88.
47. Sims TN, et al. (2007) Opposing effects of PKCtheta and WASp on symmetry breaking and relocation of the immunological synapse. *Cell* 129(4):773–785.